



## Abstract

Many complex systems on the Earth surface show non-equilibrium fluctuations, often determining the spontaneous evolution towards a critical state. In this context salt marshes are characterized by complex patterns both in geomorphological and ecological features, which often appear to be strongly correlated.

A striking feature in salt marshes is vegetation distribution, which can self-organize in patterns over time and space. Self-organized patchiness of vegetation can often give rise to power law relationships in the frequency distribution of patch sizes. In cases where the whole distribution does not follow a power law, the variance of scale in its tail may often be disregarded. To this end, the research aims at how changes in the main climatic and hydrodynamic variables may influence such non-linearity, and how numerical thresholds can describe this. Since it would be difficult to simultaneously monitor the presence and typology of vegetation and channel sinuosity through in situ data, and even harder to analyze them over medium to large time-space scales, remote sensing offers the ability to analyze the scale invariance of patchiness distributions.

Here, we focus on a densely vegetated and channelized salt marsh (Scheldt estuary Belgium–the Netherlands) by means of the sub-pixel analysis on satellite images to calculate the non-linearity in the values of the power law exponents due to the variance of scale. The deviation from power laws represents stochastic conditions under climate drivers that can be hybridized on the basis of a fuzzy Bayesian generative algorithm.

The results show that the hybrid approach is able to simulate the non-linearity inherent to the system and clearly show the existence of a link between the autocorrelation level of the target variable (i.e. size of vegetation patches), due to its self-organization properties, and the influence exerted on it by the external drivers (i.e. climate and hydrology).

Considering the results of the stochastic model, high uncertainties can be associated to the short term climate influence on the saltmarshes, and the medium-long term spatial and temporal trends seem to be dominated by vegetation with its evolution in

# ESURFD

1, 1061–1095, 2013

## Spatial and temporal pattern analysis of salt marsh evolution

A. Taramelli et al.

Title Page

Abstract

Introduction

Conclusions

References

Tables

Figures



Back

Close

Full Screen / Esc

Printer-friendly Version

Interactive Discussion





scale-invariant power law (Bak and Chen, 1991) where fractal statistics are applicable (Malinverno, 1990; Turcotte, 1992).

Recent modeling and computer simulations lead to the conclusion that self-organization theory in mud flat, could be stochastic only if the individual element of the system are related to small changes perturbation that undergo continuously to adjustment (Weerman et al., 2010). The spatial self-organization shows to be inhibited by the top-down control within a well-behaved curve representing the dependence of one parameter to the others (Weerman et al., 2011), establishing the rapid changes in the whole landscape.

Many of the recent advances in this research field hinge on the ideas and quantitative tools, like space-borne data (Dadson, 2010; Murray et al., 2009; Taramelli and Melelli, 2009; Taramelli, 2011; Tolomei et al., 2013). In particular the analysis of the spatial distribution of vegetation pattern sizes can make use of a powerful method to characterize vegetation clusters over the broad range of spatial scales in which they occur (Scanlon et al., 2007; Taramelli et al., 2013b), like Spectral Mixture Analysis (SMA – Small, 2004). SMA classifies individual mixed pixels according to the distribution of spectrally pure endmember fractions (Taramelli et al., 2012, 2013a; Valentini, 2013) leading to a vegetation cluster definition. The inverse relation between the defined cluster size using SMA and the frequency, at which clusters of that size are found, can give rise to a power law distribution (Clauset et al., 2009; Taramelli et al., 2013b). Ecological variables owe much of their dynamic properties to the high dependence on the surrounding environmental conditions, mainly determined by physical and chemical variables; when the effect of these variables assumes considerable importance, the power law approach may be insufficient to describe ecosystem dynamics.

In this paper we show that, on certain occasions, the actual distribution does not follow a power law for all its values: in the tail of the distribution, data may lie outside of a model power law relationship and show a non-linearity, in other words a variance in the scale invariance. If patches are found to lie outside and deviate from the power law relationship, they are usually considered as statistical anomalies: as a consequence,

# ESURFD

1, 1061–1095, 2013

## Spatial and temporal pattern analysis of salt marsh evolution

A. Taramelli et al.

Title Page

Abstract

Introduction

Conclusions

References

Tables

Figures



Back

Close

Full Screen / Esc

Printer-friendly Version

Interactive Discussion



## Spatial and temporal pattern analysis of salt marsh evolution

A. Taramelli et al.

Title Page

Abstract

Introduction

Conclusions

References

Tables

Figures

⏪

⏩

◀

▶

Back

Close

Full Screen / Esc

Printer-friendly Version

Interactive Discussion



the non-linearity in the power law tail may often be disregarded. To address this issue, in this paper we hybridize a power law approach with a fuzzy naïve Bayesian classification algorithm, in order to (a) identify the possible nonlinearity thresholds in vegetation patch sizes, (b) to quantify the change of scale in the distribution and (c) to investigate the specific properties of the non-linear tail of the distribution.

Naive Bayes classifiers are an old and well-known type of classifiers that assign a class from a predefined set to an object or case under consideration based on the values of descriptive attributes. An intuitive approach to deal with regions of higher and lesser data point density, where the boundaries between the clusters can only be drawn with a certain amount of arbitrariness, is to make it possible that a data point belongs in part to one cluster, in part to a second etc. Fuzzy cluster analysis has the requirement that a data point must not be assigned to exactly one cluster but it allows gradual memberships (Bezdek, 1981; Bezdek and Pal, 1992).

The analytical approach in the present study allows to deal with tide-dominated environments described as pulsing steady state (Odum et al., 1995), in which the pulse inside the target variable is largely dependent on intermittent external dynamics, namely the pulsing water flow regime or hydroperiod. The hybrid approach between power laws and fuzzy naïve Bayes inference, which is potentially able to define the trajectory covered in the shift between two basins of attraction, represent the evolution of vegetation patches and channel sinuosity that can be used to forecast potential deviation taking into account the climatic and hydrological regimes.

## 2 Study area

The case study to test the methodology is a salt marsh environment, where strong interactions between organisms and the environment are particularly evident. Here we examine the spatial and temporal dynamics of the Saeftinghe salt marsh in the Scheldt estuary, at the Dutch–Belgian border. Tidal influence is dominant over the whole estuary and in the lower parts of some tributaries. Tidal excursion is variable within the

estuary, since there are different volumes of water transported. In the portion of the mouth, near Vlissingen, the average tidal range is 3.8 m (between the 2.81 m at neap and 4.85 m at spring tide).

The area, comprising approximately 30 km<sup>2</sup> and being one of the largest marshes in Europe, is dominated by tidal influence. On the basis of the salinity gradient in the estuary, the study area considered in this work is located in the brackish portion. The two-way interactions between biological and physical processes are particularly evident in Saeftinghe: in the 30's, only 25 % of the area was covered by salt marsh vegetation, while the rest consisted of mudflats and tidal channels (Vandenbruwaene et al., 2012). As of today, the proportions are exactly reversed: Saeftinghe is formed by 30 % of mudflats and channel systems, while the remaining 70 % of the surface is covered by salt marsh vegetation. In Saeftinghe, stands of climax common reed *Phragmites australis* can be found. *Elymus athericus* is the dominant species of Saeftinghe, is an upper-marsh grass, a competitive species for its ability in nitrogen assimilation. Patches of *Spartina anglica*, *Salicornia europaea*, and to a lesser extent colonize the pioneer zone by *Scirpus maritimus* and *Puccinellia maritima*.

This relatively rapid increase in vegetation, as well as the strong climate and hydrological forcing to which it is subject, make Saeftinghe an ideal setting to explore the spatio-temporal dynamics of salt marshes (Taramelli et al., 2013a).

### 3 Data and methodology

The remotely sensed dataset was composed by a total of 18 Landsat Thematic Mapper (Table 1) and Enhanced Thematic Mapper (Table 2) optical multispectral images (US Geological Survey, 2003), spanning from 1984 to 2011 (Table 3). Surface characteristics of the Saeftinghe salt marsh were mapped using SMA, and a decision tree classifier was employed to obtain a final classification map. SMA was used to map vegetation cover classes, as well as the calculation of channel network sinuosity.

## Spatial and temporal pattern analysis of salt marsh evolution

A. Taramelli et al.

Title Page

Abstract

Introduction

Conclusions

References

Tables

Figures



Back

Close

Full Screen / Esc

Printer-friendly Version

Interactive Discussion



### 3.1 Vegetation mapping and patch size calculation

The two-dimensional spatial structure of vegetation was characterized by the size-frequency distribution of contiguous pixels showing the same typology of vegetation cover. SMA was used to identify the presence of patches that occur at sizes that go below the pixel resolution of Landsat imagery (30 m by 30 m), such as the ones in the pioneer zone. We discriminated between a low-pioneer vegetation, a high vegetation dominated by *Elymus athericus* and the reed stands of *Phragmites australis* by classifying the mixed pixels in the abundance fraction maps. We then applied a threshold to fraction cover values, to obtain binary matrices of presence/absence for each class. We defined patch boundaries on the basis of the connectivity of each vegetation pixel to its four neighboring pixels (von Neumann neighborhood algorithm). For each patch, its area was calculated to test the plausibility of the power law distribution.

### 3.2 Channel sinuosity calculation

Similarly to marsh vegetation patterns, channel network was extracted from fraction maps, with the difference that in this case the processing started by using the “dark” endmember. Channel fraction maps were converted into binary presence/absence images based on a threshold fraction value. The reclassified image was then imported in Matlab for the network extraction through the skeletonization algorithm (Gonzalez et al., 2004). This morphological operation is used on binary images to reduce each component to the thickness of a single row of pixels and to obtain the object’s skeleton, preserving the original shape and connectivity. The algorithm was repeated until further reiterations did not bring any changes to the skeleton structure.

The degree of meandering of the channel network was then measured quantitatively through the calculation of channel sinuosity. Sinuosity  $s = l/L$  is the ratio between the along-stream length  $l$  to the straight-line distance  $L$  between the starting and ending points (the two nodes of each channel). Branch points (points of channel bifurcation) were detected and subtracted from the channel network skeleton to obtain isolated

## Spatial and temporal pattern analysis of salt marsh evolution

A. Taramelli et al.

Title Page

Abstract

Introduction

Conclusions

References

Tables

Figures



Back

Close

Full Screen / Esc

Printer-friendly Version

Interactive Discussion



branches. We calculated along-path distance  $l$  for each skeletonized branch, while straight-line distance  $L$  between endpoints was calculated using Pythagoras' theorem. Finally, sinuosity was computed as the ratio between the two values.

Channel network attributes used as input variables in the model are (i) the number of bifurcation points, (ii) the total number of channels, (iii) average channel sinuosity for each remote sensing acquisition.

### 3.3 Hydrological and climatic data

The training dataset used for the model also comprises a series of in situ hydrological and climatic data. The variables used to describe the environmental boundary conditions are (i) salinity, (ii) high water level, (iii) rainfall, (iv) tide level at the time of image acquisition, each of them averaged over different time spans (14, 30 and 60 days before each remote sensing acquisition). Salinity was measured at the reference station of Baal, water and tidal levels at the station of Bath, and daily historical precipitation amounts were collected from the meteorological station of Kloosterzande. The three stations are located in the Netherlands, close to the Saeftinghe marsh (see Fig. 1).

### 3.4 Power law

We started from the fact that the aspect of actual landscapes does not correspond to a “dynamic equilibrium”, but to a self-organized order at the edge of chaos in an open dissipative system. As already summarized by Scheidegger (1994) “in a fractal set of dimension  $D$ , there exists a power law of subsets: the number  $N$  of subsets of linear size  $D$  is proportional to  $L^{-D}$ . In terms of size ( $M$ )-frequency ( $N$  number of events per unit time) distributions, the power law mentioned is represented by a Gutenberg and Richter (1949), type law:

$$\text{Log } N(M) = a - bM \quad (1)$$

which is a power law for  $N$ .”

## Spatial and temporal pattern analysis of salt marsh evolution

A. Taramelli et al.

Title Page

Abstract

Introduction

Conclusions

References

Tables

Figures

◀

▶

◀

▶

Back

Close

Full Screen / Esc

Printer-friendly Version

Interactive Discussion



## Spatial and temporal pattern analysis of salt marsh evolution

A. Taramelli et al.

Title Page

Abstract

Introduction

Conclusions

References

Tables

Figures

⏪

⏩

◀

▶

Back

Close

Full Screen / Esc

Printer-friendly Version

Interactive Discussion



Such power laws have been found everywhere in self-ordered natural system (Hoff and Bevers, 1998; Malinverno, 1990; Stark and Hovius, 2001; Stark and Guzzetti 2009). But as the natural systems are not linear and not following the growth equation of the type Eq. (1), they usually follow a logistic equation like (Cambel, 1993; Scheidegger, 1994):

$$dx(t)/dt = rx(t)[1 - x(t)] \quad (2)$$

where  $x$  is a normalized deviation-variable and  $r$  a system parameter.

Its solution is (Scheidegger, 1994)

$$x(t) = 1/[1 + \exp(-rt)] \quad (3)$$

Based on the vegetation pattern areas defined in Sect. 3.1, we calculated the size-frequency distribution of patch size and we investigated whether the relationship could be described by a power law. If a deviation from the model distribution was found to occur in the power law tail, we considered that patch size as a non-linearity threshold, and another power law was calculated only for the values in the tail that exceeded that threshold.

We fitted the power law to the data using the methods implemented by Clauset et al. (2009), through which we estimated  $\alpha$  and the lower limit of observed power law behavior,  $x_{\min}$ , using the method of maximum likelihood.

### 3.5 Fuzzy naïve Bayes approach

The high complexity and uncertainty associated with ecological systems under power law tail, can be then treated using a combination of fuzzy logic and a naïve Bayes compiler. As in ordinary naïve Bayes, the compiler processes the data to estimate the parameters in the form of instances.

The compiler algorithm consists of the following five steps (Widyantoro and Yen, 2000):

## Spatial and temporal pattern analysis of salt marsh evolution

A. Taramelli et al.

Title Page

Abstract

Introduction

Conclusions

References

Tables

Figures

◀

▶

◀

▶

Back

Close

Full Screen / Esc

Printer-friendly Version

Interactive Discussion



1. fuzzyfication of the variables
2. learning phase
3. fuzzy naïve Bayes inference on the new observed instances
4. definition of the result using the centroid rule within the uncertainty interval resulting from the compiler
5. defuzzyfication of the output.

1 – Fuzzyfication of the variables: it consists in the expression of the original variables according to fuzzy formalism. A fuzzy partitioning is generated within the domain of values of each variable, for which each domain of the system is described using a series of fuzzy sets (Taramelli and Melelli, 2008; Gazzea et al., 2009). In particular, in this case we used isosceles triangle-shaped membership functions for their characteristics of computational simplicity and objectivity. The domain of existence of each variable was first standardized in the range 0–100 and then partitioned into 6 triangular fuzzy sets with the same amplitude, according to which we fuzzyfied the observations of the training set.

2 – Learning phase: during this phase, the system estimates the classifier parameters, deriving them from both the marginal and conditioned probabilities of each fuzzy set. The marginal probabilities are calculated through the equation:

$$P(x_i) = \frac{\left( \sum_{e \in L} \mu_{x_i}^e \right) + 1}{|L| + |\text{dom}(x_i)|} \quad (4)$$

Where  $L$  is the learning set,  $\text{dom}(x_i)$  is the domain of the  $i$ th fuzzy set of the variable  $x$ , and  $e$  indicates a generic instance of the learning set  $L$ , while the conditional

probabilities are calculated through the equation:

$$P(x_i|y) = \frac{\left( \sum_{\theta \in L} \mu_{x_i}^{\theta} \mu_y^{\theta} \right) + 1}{\left( \sum_{\theta \in L} \mu_{x_i}^{\theta} \right) + |\text{dom}(x_i)|} \quad (5)$$

In the “learning phase”, both the joint and the conditioned probability values are calculated according to the definition of Lebesgue’s probability space and refer to the fuzzy event, that is to say to the possibility that a given variable is getting values numbered in a particular fuzzy set (Zadeh, 1968).

3 – Fuzzy naïve Bayes inference: given an observed, foreseen or simulated new instance, the compiler calculates the probability of each fuzzy set of the target variable, conditioned upon the new observed instance:

$$P(y|e) = P(y) \left( \sum_{x \in X_i} \frac{P(x_i|y)}{P(x_i)} \mu_{x_i}^e \right) \dots \left( \sum_{x \in X_n} \frac{P(x_n|y)}{P(x_n)} \mu_{x_n}^e \right) \quad (6)$$

The final output of the target variable will be a series of conditional probabilities associated to the target fuzzy sets.

4 – The resultant values are obtained according to the maximum a posteriori probability (MAP) rule through the centroid mode of operation. This will give one or more values according to the more or less high degree of probability associated to the new instances, on the basis of the statistical similarity to the training instances.

### 3.6 Hybridization

The combined utilization of the fuzzy logic and naïve-Bayes classifier provides a classification output, which is very close to being as accurate as the output of a predictive methodology. The domain of the output (target) variable, which has undergone

## Spatial and temporal pattern analysis of salt marsh evolution

A. Taramelli et al.

Title Page

Abstract

Introduction

Conclusions

References

Tables

Figures

⏪

⏩

◀

▶

Back

Close

Full Screen / Esc

Printer-friendly Version

Interactive Discussion



fuzzyfication, is represented by indistinct classes so that the domain is continuous with respect to the possible values of described variable.

The power law non linearity was then hybridized with a fuzzy naïve Bayesian classification algorithm, in order to identify the patch sizes of the nonlinearity thresholds in the tail, to quantify the change of scale in the distribution and investigate its specific properties. The methodology is concerned with the prediction of the values at which environmental variables may lead the system towards a nonlinearity threshold. The identification of such threshold through simulations may then be used in the monitoring phase of intertidal marshes.

We developed a nested fuzzy Bayesian model consisting of three steps, in each of which we estimated a different target variable. The model was applied in a nested way to enter the complex structure of the system by increasing, run after run, the degree of complexity of the target variable. Only one of the three vegetation classes – the “High” vegetation dominated by *Elymus athericus* – was used as target variable to test the model. This choice was made to obtain a more consistent dataset, using a class in which the deviations in the power law tails were more frequently observed: this way, we explored all three steps of the nested model with a sufficiently large number of samples.

To achieve the desired level of complexity, we performed a first fuzzy Bayesian modeling in which the target variable was the patch size corresponding to a deviation from the linear logarithmic relationship. The patch size was quantified as the quantile of the distribution at which the emergence of a nonlinearity is most likely to occur. This first step is estimated using the average salinity, high water levels and rainfall measurements observed before each image acquisition.

Along with the variables already used in the first model, the results of the first run become the input of the second one. Within the tail of the distribution the target for the nested fuzzy Bayesian model variable becomes the power law exponent.

In reaching a greater level of complexity, the outputs of the first two steps and the channel network properties (sinuosity and number of bifurcation points – Taramelli

# ESURFD

1, 1061–1095, 2013

## Spatial and temporal pattern analysis of salt marsh evolution

A. Taramelli et al.

Title Page

Abstract

Introduction

Conclusions

References

Tables

Figures



Back

Close

Full Screen / Esc

Printer-friendly Version

Interactive Discussion



et al., 2013b) have been used as input for the final, third step, to estimate the inundated salt marsh area for a given tidal level.

The final classification is not therefore absolute but it specifies an uncertainty range within the continuous domain of the target variable. Inside this uncertainty range, the centroid rule determines a punctiform prevision with accuracy comparable to a deterministic prevision. The amplitude of the uncertainty range, within which the classification falls, is a function of the original fuzzy partitioning and of the statistical likelihood between the training data set and the new calculated instances.

## 4 Results

The patch sizes calculated for the whole time series (18 images between 1984 and 2011), using the binary images of vegetation presence/absence, have been plotted by ranking the patch size classes from the smallest to the largest (Fig. 2). This diagram clearly shows the overall consistency of a power law relationship and confirms the general higher frequency of smaller patches.

By comparing patch sizes and the main typology of vegetation for each patch size, we observed how the variety of vegetation typologies varies as a function of the patch size (Fig. 3). The lower sizes of the distribution represent the higher level of diversity in patch typology, with a dominance of high and dense stands of *Elymus athericus* vegetation. In fact, with increasing patch sizes, there is a decrease in the variety of vegetation typologies until, after a certain size, patches become monospecific. The dashed line in Figs. 2 and 3 indicates this threshold, relative to the largest patches and equal to 2245 pixels.

Observing the channel network characteristics across the salt marsh (Fig. 4), the higher sinuosity values can be found around the smaller patches, while a lower number of channels seem to develop near the larger ones. Although some fluctuations are found in average sinuosity values along the time series, the average for the 18 Landsat images is  $1.08 \pm 0.016$ .

## Spatial and temporal pattern analysis of salt marsh evolution

A. Taramelli et al.

Title Page

Abstract

Introduction

Conclusions

References

Tables

Figures



Back

Close

Full Screen / Esc

Printer-friendly Version

Interactive Discussion





less precise, but still the model is able to calculate uncertainty ranges that closely fit the target variable.

The uncertainty associated with each result is the range of values of the target variable with the highest probability of occurrence. In fact, the model output is not a series of point values, but rather ranges of equally likely values. The width of the interval is determined by the similarity between the classified instance and the training data, on which we carried out the learning phase of the model. The fuzzy naïve Bayes uncertainty thus indicates the output accuracy, based on the data on which the stochastic model has *learned* the deterministic/empirical parameters of the system to be modeled. The nature of this uncertainty implies the possibility to improve the accuracy of the simulations, by adjusting the amount of information in the parameter estimation and the fuzzy partition used in data processing and in the simulations. Another important consequence of the MAP (maximum a posteriori probability) uncertainty is the ability to continuously recalibrate the model parameters in order to *chase* the uncertainty expanding within the system, especially when extreme drivers or unobserved values are present. Therefore, the range of uncertainty describes the *confidence* of the model in the results it has produced and the similarity between the learning instances and the instances used for the simulations. Consequently, it indicates the variability that can be observed in the system in response to the drivers used in the simulations.

The estimation of non-linearity thresholds, inferred from the observed vegetation patch size distributions, can be used to describe the emergence of another power law relationship in the tail of the distribution. This is because the errors in each estimate are strictly asymmetrically distributed biasing any regression fit in the whole original power law distribution which assumes only normally distributed errors. Smoothing hides any crossover from non-power-law scaling to a power law induced by the application of the fuzzy-Bayesian approach that can justify and explain the non-linear relationship observed between the percentage of inundated salt marsh area and the tidal level in the third step (Fig. 8). In this step, leading to the estimation of the percentage of inundated salt marsh area, the model runs into a non-linearity threshold beyond which

**Spatial and temporal pattern analysis of salt marsh evolution**

A. Taramelli et al.

Title Page

Abstract

Introduction

Conclusions

References

Tables

Figures



Back

Close

Full Screen / Esc

Printer-friendly Version

Interactive Discussion



## Spatial and temporal pattern analysis of salt marsh evolution

A. Taramelli et al.

Title Page

Abstract

Introduction

Conclusions

References

Tables

Figures



Back

Close

Full Screen / Esc

Printer-friendly Version

Interactive Discussion



the response of the target variable (here inundation time) shows different dynamics related to changes of the ecosystem state that the tail in the power law was highlighting (Fig. 8). This reveals a non-linearity in forecasting the evolution of the response variable. The threshold appears to be at around  $-50$  cm NAP and at  $95$  cm NAP. Therefore for a potential change in external environmental variables – in this case the tidal level and hydroperiod – the corresponding variations in overflowed salt marsh area may be accurately predicted using the tail of the power law.

It is important to note that pairwise correlations between each target and the single environmental variables were not enough to accurately describe the phenomenon in question (see Table 4). This result stresses the limitations of using variables alone to describe intertidal systems, and at the same time it confirms the importance of using a more complex approach, such as the one presented in this paper.

## 5 Discussion

The applied non-linear power law shows a high dependence of the detected vegetation patchiness on the surrounding environmental conditions (salinity, rainfall, water height). The simulations clearly show the existence of a link between the autocorrelation level of the target variable (vegetation), due to its self-organization properties, and the influence exerted on it by the external drivers. The hybrid approach is able to simulate the non-linearity inherent to the system, which would otherwise be undetectable from a classic power law approach that can individually characterize only a part of the stochasticity of the system.

The results are in agreement with the theory of complex systems, in which the system dynamics are influenced by emergent behaviors that cannot be described by single variables but by their synergistic interaction. In particular, the phenomenon of emergent behavior is related to the power law distribution of vegetation patches for which, in some cases, the points do not seem to thoroughly follow the power law that they themselves have generated. It should be noted that even the points that appear not



## Spatial and temporal pattern analysis of salt marsh evolution

A. Taramelli et al.

Title Page

Abstract

Introduction

Conclusions

References

Tables

Figures

◀

▶

◀

▶

Back

Close

Full Screen / Esc

Printer-friendly Version

Interactive Discussion



estimation of the power-law scaling considering larger surge events on the size of the vegetation patches. The scaling suggests that the areas disturbed by different patches of vegetation are linked to the sinuosity yield, and are essentially reliant on the frequency of smaller surge/rain. Other results also indicate that the probability of extreme events is less than previous studies would predict (Taramelli et al., 2013b). The –50 and +95 cm thresholds indicate, in fact, the state case where the amount of flooding is more variable and should depend more on the climate of the daily rates of rain, added to tide levels. Less rainy days drives mudflats to surficial dryness and cohesiveness, especially in small patches where the higher salinity and vegetation thirsty determines scarce water uptake, while after rainy days, mud is less cohesive and plants less thirsty can dedicate themselves to the growth of both stands and roots so that, the increased sediment transport and deposition increase the size of the intermediate and large patches. The flood, as observed from fuzzy Bayes model could have a greater effect on smaller patches that are subject to pulse and continuous disturbance (tide) but at the same, they are especially encouraged to leave the steady state because often more influenced by the abrupt changes (but not extreme) of water level, salinity and sediment deposition. That is, the small patches suffer the daily effect of the climate and its changes. They deliver to the patches, variable amounts of water making them exposed to more stable conditions in term of size and sinuosity. Here vegetation is stable, advances and collaborates with the sediment.

## 6 Conclusions

Tide-dominated ecosystems, regulated by the pulsing of the water flow regime, have been shown to be well suited for a hybrid approach between power laws and a fuzzy naïve Bayes algorithm, which is potentially able to describe the ecosystem's state and evolution in response to external dynamics.

The joint approach was able to add a specific component of non-linearity in the power laws, in the level of complexity reached by the external environmental variables. The



## Spatial and temporal pattern analysis of salt marsh evolution

A. Taramelli et al.

Title Page

Abstract

Introduction

Conclusions

References

Tables

Figures

◀

▶

◀

▶

Back

Close

Full Screen / Esc

Printer-friendly Version

Interactive Discussion



- Dadson, S.: Geomorphology and Earth system science, *Prog. Phys. Geog.*, 34, 385–398, 2010.
- D'Alpaos, A., Lanzoni, S., Marani, M., Fagherazzi, S., and Rinaldo, A.: Tidal network ontogeny: channel initiation and early development, *J. Geophys. Res.-Earth*, 110, F02001, doi:10.1029/2004JF000182, 2005.
- 5 Gazzea, N., Taramelli, A., Valentini, E., Piccione, E.: Integrating fuzzy logic and GIS analysis to assess sediment characterization within a confined harbour, *Lectures Notes in Computer Sciences*, 5592, 33–49, 2009.
- Gonzalez, R. C., Woods, R. E., and Eddins, S. R.: *Digital Image Processing using MATLAB*, Pearson Prentice Hall, New Jersey, 2004.
- 10 Gutenberg, B. and Richter, C. F.: *Seismicity of the Earth and associated phenomena*, Princeton University Press, Princeton, New Jersey, 1949.
- Hoff, J. and Bevers, M. (Eds.): *Spatial Optimization for Managed Ecosystems*, Columbia University Press, New York, 258 pp., 1998.
- 15 Kéfi, S., Rietkerk, M., Alados, C. L., Pueyo, Y., Papanastasis, V. P., EIAich, A., and De Ruiter, P. C.: Spatial vegetation patterns and imminent desertification in Mediterranean arid ecosystems, *Nature*, 449, 213–217, 2007.
- Maiti, S. and Bhattacharya, A. K.: Shoreline change analysis and its application to prediction: a remote sensing and statistics based approach, *Mar. Geol.*, 257, 11–23, 2009.
- 20 Malinverno, A.: A simple method to estimate the fractal dimension of a self-affine series, *Geophys. Res. Lett.*, 17, 1953–1956, 1990.
- Marani, M., Lanzoni, S., Zandolin, D., Seminara, G., and Rinaldo, A.: Tidal meanders, *Water Resour. Res.*, 38, 1–14, 2002.
- Murray, A. B., Lazarus, E., Ashton, A., Baas, A., Coco, G., Coulthard, T., Fonstad, M., Haff, P., 25 McNamara, D., and Paola, C.: Geomorphology, complexity, and the emerging science of the Earth's surface, *Geomorphology*, 103, 496–505, 2009.
- Odum, W. E., Odum, E. P., and Odum, H. T.: Nature's pulsing paradigm, *Estuaries*, 18, 547–555, 1995.
- Rietkerk, M. and van de Koppel, J.: Regular pattern formation in real ecosystems, *Trends Ecol. Evol.*, 23, 169–175, 2008.
- 30 Rigon, R., Rinaldo, A., and Rodriguez-Iturbe, I.: On landscape self-organization, *J. Geophys. Res.-Sol. Ea.*, 99, 11971–11993, 1994.

## Spatial and temporal pattern analysis of salt marsh evolution

A. Taramelli et al.

Title Page

Abstract

Introduction

Conclusions

References

Tables

Figures

◀

▶

◀

▶

Back

Close

Full Screen / Esc

Printer-friendly Version

Interactive Discussion



- Scanlon, T. M., Caylor, K. K., Levin, S. A., and Rodriguez-Iturbe, I.: Positive feedbacks promote power-law clustering of Kalahari vegetation, *Nature*, 449, 209–212, 2007.
- Scheidegger, A. E.: The principle of antagonism in the earth's evolution, *Tectonophysics*, 55, T7–T10, 1979.
- 5 Scheidegger, A. E.: Instability principle in geomorphic equilibrium, *Z. Geomorphol.*, 30, 257–273, 1983.
- Scheidegger, A. E.: The fundamental principles of landscape evolution, *Catena suppl.*, 10, 199–210, 1987.
- Scheidegger, A. E.: Hazards: singularities in geomorphic systems, *Geomorphology*, 10, 19–25, 10 1994.
- Singer, R. B. and McCord, T. B.: Mars-large scale mixing of bright and dark surface materials and implications for analysis of spectral reflectance, *Lunar and Planetary Science Conference Proceedings*, 1835–1848, 1979.
- Small, C.: Estimation of urban vegetation abundance by spectral mixture analysis, *Int. J. Remote Sens.*, 22, 1305–1334, 2001.
- 15 Small, C.: The Landsat ETM+ spectral mixing space, *Remote Sens. Environ.*, 93, 1–17, 2004.
- Stark, C. P. and Guzzetti, F.: Landslide rupture and the probability distribution of mobilized debris volumes, *J. Geophys. Res.*, 114, F00A02, doi:10.1029/2008JF001008, 2009.
- Stark, C. P. and Hovius, N.: The characterization of landslide size distributions, *Geophys. Res. Lett.*, 28, 1091–1094, 2001.
- 20 Stark, C. P. and Stieglitz, M.: Hydrology: The sting in a fractal tail, *Nature*, 403, 493–495, 2000.
- Taramelli, A.: Detecting landforms using quantitative radar roughness characterization and spectral mixing analysis, in: *Geocomputation, Sustainability & Environ. Planning*, SCI 348, edited by: Murgante, B., Borruso, G., and Lapucci, A., 225–249, 2011.
- 25 Taramelli, A. and Melelli, L.: Detecting alluvial fans using quantitative roughness characterization and fuzzy logic analysis, *Lectures Notes in Computer Sciences*, 5072, 1–15, 2008.
- Taramelli, A. and Melelli, L.: Map of deep seated gravitational slope deformations susceptibility in central Italy derived from SRTM DEM and spectral mixing analysis of the Landsat ETM+ data, *Int. J. Remote Sens.*, 30, 357–387, 2009.
- 30 Taramelli, A., Giardino, C., Gasperini, L., del Bianco, F., Bresciani, M., Valentini, E., Pizzimenti, L., Zucca, F., and Disperati, L.: Biophysical and morphological study of coastal habitats from imaging spectrometry, LIDAR and in situ data acquisition, *The hyperspectral workshop 2010*, ESRIN 17–19 March 2010, Frascati, 2010.

## Spatial and temporal pattern analysis of salt marsh evolution

A. Taramelli et al.

Title Page

Abstract

Introduction

Conclusions

References

Tables

Figures

◀

▶

◀

▶

Back

Close

Full Screen / Esc

Printer-friendly Version

Interactive Discussion



- Taramelli, A., Valentini, E., Dejana, M., Zucca, F., and Mandrone, S.: Modelling coastal processes by means of innovative integration of remote sensing time series analysis, in: 2011 IEEE International Geoscience and Remote Sensing Symposium Proceedings, Vancouver, British Columbia, Canada, 24–29 July 2011, 1547–1550, 2011.
- 5 Taramelli, A., Pasqui, M., Barbour, J., Kirschbaum, D., Bottai, L., Busillo, C., Calastrini, F., Guarnieri, F., and Small, C.: Spatial and temporal dust source variability in northern China identified using advanced remote sensing analysis, *Earth Surf. Proc. Land.*, 38, 793–809, doi:10.1002/esp.3321, 2013.
- Taramelli, A., Valentini, E., Cornacchia, L., Mandrone, S., Monbaliu, J., Hoggart, S. P. G., Thompson, R. C., and Zanuttigh, B.: Modelling uncertainty in estuarine system by means of combined approach of optical and radar remote sensing, *Coast. Eng.*, doi:10.1016/j.coastaleng.2013.11.001, in press, 2013a.
- 10 Taramelli, A., Valentini, E., Cornacchia, L., Monbaliu, J., and Sabbe, K.: Self-organized processes between salt marsh vegetation patterns and channel network in a tidal landscape, *J. Geophys. Res.*, submitted, 2013b.
- Taylor, G. I.: The instability of liquid surfaces when accelerated in a direction perpendicular to their planes, *Proc. R. Soc. Lond. Ser. A.*, 201, 192–196, 1950.
- Temmerman, S., Bouma, T., Van de Koppel, J., Van der Wal, D., De Vries, M., and Herman, P.: Vegetation causes channel erosion in a tidal landscape, *Geology*, 35, 631–634, 2007.
- 20 Terjung, W. H.: *Process-Response Systems in Physical Geography*, Dümmler, Bonn, 1982.
- Tolomei, C., Taramelli, A., Moro, M., Saroli, M., Salvi, S.: Analysis of DGSD impending over the Fiastra lake (Central Italy), by geomorphological assessment and deformation monitoring using satellite SAR Interferometry, *Geomorphology*, 201, 281–292, doi:10.1016/j.geomorph.2013.07.002, 2013.
- 25 Turcotte, D.: *Fractals and Chaos in Geology and Geophysics*, Cambridge University Press, New York, 1992.
- US Geological Survey: Landsat: a global land-observing program, Fact Sheet 023-03, available at: <http://egsc.usgs.gov/isb/pubs/factsheets/fs02303.html>, 2003.
- Valentini, E.: A new paradigm in coastal ecosystem assessment: linking ecology and geomorphology implementing the FHyL approach, Ph.D. thesis, University of Tuscia, Italy, 2013.
- 30 Vandenbruwaene, W., Bouma, T. J., Meire, P., and Temmerman, S.: Bio-geomorphic effects on tidal channel evolution: impact of vegetation establishment and tidal prism change, *Earth Surf. Proc. Land.*, 38, 122–132, doi:10.1002/esp.3265, 2012.

- Weerman, E. J., Herman, P. M. J., van de Koppel, J.: Top-down control inhibits spatial self-organization of a patterned landscape, *Am. Nat.*, 176, 487–495, doi:10.1086/652991, 2010.
- Weerman, E. J., van de Koppel, J., Eppinga, M. B., Montserrat, F., Liu, Q.-X., Herman, P. M. J.: Spatial self organization on intertidal mudflats through biophysical stress divergence, *Ecology*, 92, 487–495, 2011.
- 5 Weerman, E. J., van Belzen, J., Rietkerk, M., Temmerman, S., Kefi, S., Herman, P. M. J., van de Koppel, J.: Changes in diatom patch-size distribution and degradation in a spatially self-organized inter tidal mudflat ecosystem, *Ecology*, 93, 608–618, 2012.
- 10 Widyantoro, D. H. and Yen, J.: A fuzzy similarity approach in text classification task, The Ninth IEEE International Conference on Fuzzy Systems, FUZZ IEEE 2000, 653–658, 2000.
- Zadeh, L. A.: Fuzzy algorithms, *Inform. Control*, 12, 94–102, 1968.

---

**Spatial and temporal pattern analysis of salt marsh evolution**A. Taramelli et al.

---

Title Page

Abstract

Introduction

Conclusions

References

Tables

Figures

◀

▶

◀

▶

Back

Close

Full Screen / Esc

Printer-friendly Version

Interactive Discussion



## Spatial and temporal pattern analysis of salt marsh evolution

A. Taramelli et al.

**Table 1.** Specifications of the Landsat Thematic Mapper (TM) sensor (US Geological Survey, 2003).

Band no.	Wavelength ( $\mu\text{m}$ )	Spatial resolution (m)
1	0.45–0.52	30
2	0.52–0.60	30
3	0.63–0.69	30
4	0.76–0.90	30
5	1.55–1.75	30
6	10.4–12.5	120
7	2.08–2.35	30

Title Page

Abstract

Introduction

Conclusions

References

Tables

Figures

◀

▶

◀

▶

Back

Close

Full Screen / Esc

Printer-friendly Version

Interactive Discussion



## Spatial and temporal pattern analysis of salt marsh evolution

A. Taramelli et al.

**Table 2.** Specifications of the Landsat Enhanced Thematic Mapper (ETM+) sensor (US Geological Survey, 2003).

Band no.	Wavelength ( $\mu\text{m}$ )	Spatial resolution (m)
1	0.45–0.515	30
2	0.525–0.605	30
3	0.63–0.69	30
4	0.75–0.90	30
5	1.55–1.75	30
6	10.4–12.5	60
7	2.09–2.35	30
8	0.52–0.9	15

Title Page

Abstract

Introduction

Conclusions

References

Tables

Figures

◀

▶

◀

▶

Back

Close

Full Screen / Esc

Printer-friendly Version

Interactive Discussion



**Spatial and temporal  
pattern analysis of  
salt marsh evolution**

A. Taramelli et al.

Title Page

Abstract

Introduction

Conclusions

References

Tables

Figures

◀

▶

◀

▶

Back

Close

Full Screen / Esc

Printer-friendly Version

Interactive Discussion

**Table 3.** List of Landsat images used.

Acquisition date	Sensor	Path	Row
20 Aug 1984	TM	199	24
10 Aug 1986	TM	199	24
23 Apr 1987	TM	199	24
9 May 1987	TM	199	24
25 May 1987	TM	199	24
14 Feb 2000	ETM	199	24
1 Aug 2000	ETM	198	24
24 Aug 2000	ETM	199	24
23 May 2001	ETM	199	24
30 Oct 2001	ETM	199	24
15 Nov 2001	ETM	199	24
8 Apr 2002	ETM	199	24
29 Jul 2002	ETM	199	24
26 Mar 2003	ETM	199	24
29 May 2003	ETM	199	24
30 Jun 2006	TM	199	24
16 Jul 2006	TM	199	24
9 Apr 2011	TM	199	24

## Spatial and temporal pattern analysis of salt marsh evolution

A. Taramelli et al.

**Table 4.** Pairwise correlations between the model target variables (patch size threshold and scaling exponent in the tails) and each environmental variable used for the fuzzy naïve Bayes inference. Mean high water level and average rainfall were averaged at different time steps (14, 30 and 60 days) before each satellite acquisition.

	Mean High Water Level			Average Rainfall			Average channel sinuosity	No. of bifurcation points
	14 d	30 d	60 d	14 d	30 d	60 d		
Patch size threshold	0.66	0.73	0.76	0.34	0.56	0.62	–	–
Scaling exponent in the tail	–0.69	–0.78	–0.69	–0.74	–0.58	–0.30	0.04	0.14

Title Page

Abstract

Introduction

Conclusions

References

Tables

Figures

◀

▶

◀

▶

Back

Close

Full Screen / Esc

Printer-friendly Version

Interactive Discussion



## Spatial and temporal pattern analysis of salt marsh evolution

A. Taramelli et al.

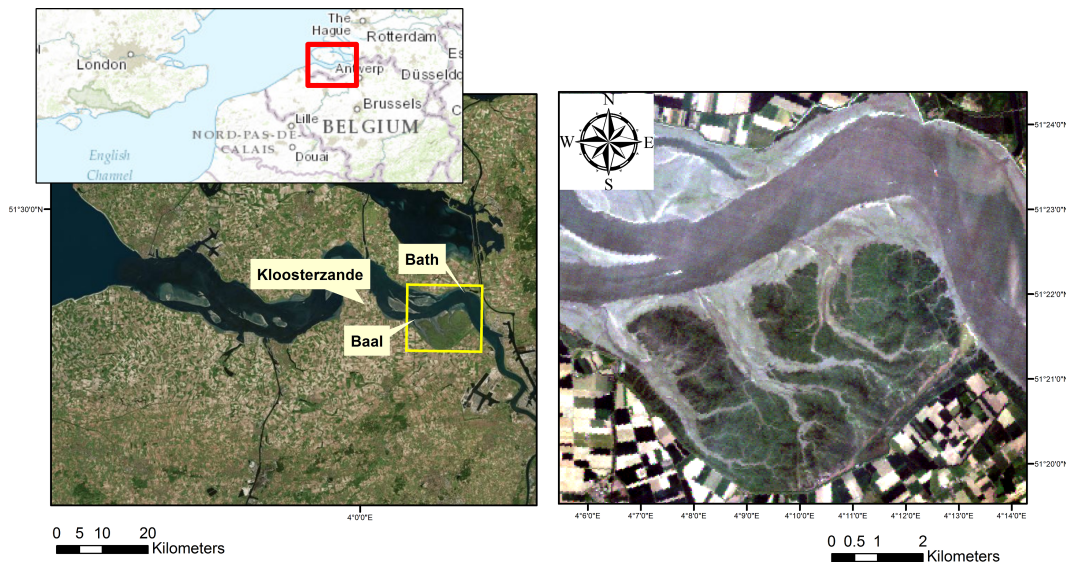


**Fig. 1.** Left: landsat satellite image of the Scheldt estuary and location of the measurement stations used in this study (see Sect. 3.3). Right: Zoom on the Saeftinghe salt marsh (R/G/B: 3/2/1, acquisition date: 26 May 2005).

**Spatial and temporal  
pattern analysis of  
salt marsh evolution**

A. Taramelli et al.

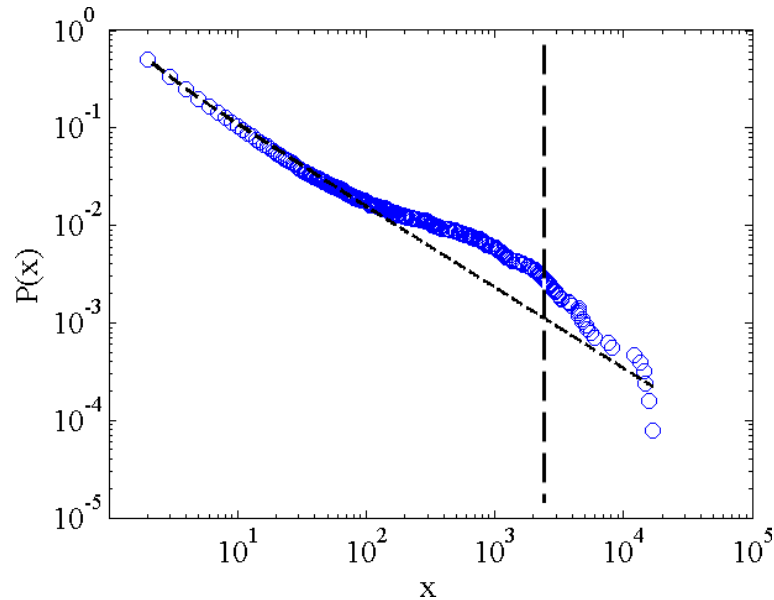


**Fig. 2.** Power law distribution for the patch sizes for the whole time series (1984–2011). The dashed line indicates the size after which patches are monospecific (represented only by the *Elymus athericus* vegetation typology).

Title Page

Abstract

Introduction

Conclusions

References

Tables

Figures

◀

▶

◀

▶

Back

Close

Full Screen / Esc

Printer-friendly Version

Interactive Discussion



## Spatial and temporal pattern analysis of salt marsh evolution

A. Taramelli et al.

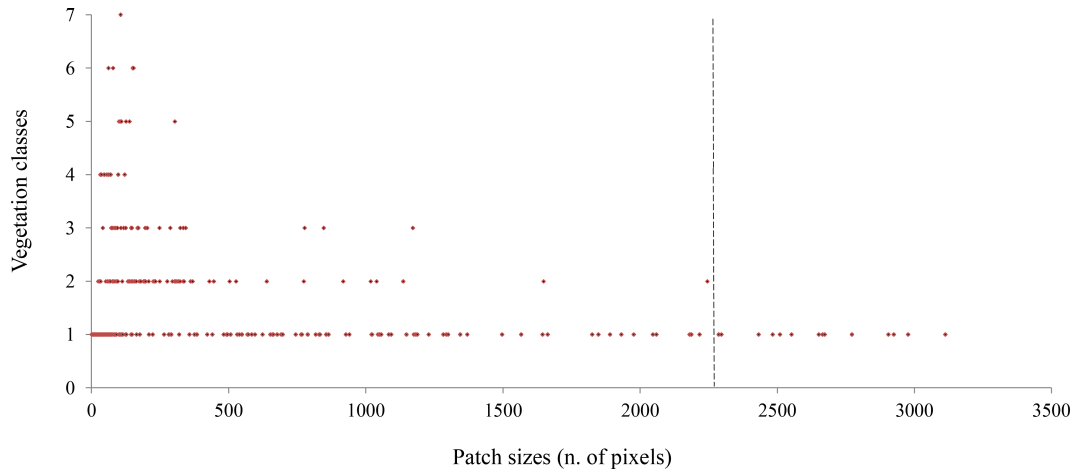


**Fig. 3.** Main vegetation typology inside each patch size. (1) High veg. (*E. athericus*), (2) Low-Pioneer, (3) Reed veg. (4) Equal frequency of Low/Pioneer-High veg. (*E. athericus*), (5) Equal frequency of Low/Pioneer-Reed veg.; (6) Equal frequency of high veg. (*E. athericus*)-Reed veg.; (7) Equal frequency for all the three classes.

Title Page

Abstract

Introduction

Conclusions

References

Tables

Figures

◀

▶

◀

▶

Back

Close

Full Screen / Esc

Printer-friendly Version

Interactive Discussion



## Spatial and temporal pattern analysis of salt marsh evolution

A. Taramelli et al.

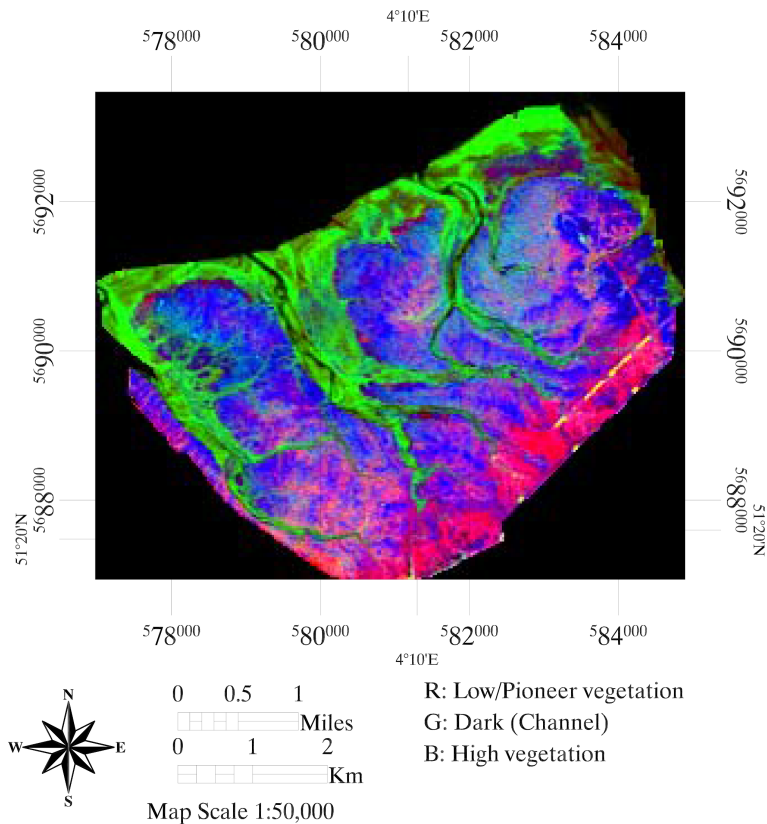


**Fig. 4.** Fraction maps for the Landsat image of 9 April 2011. The dark fraction map was used to calculate the sinuosity of the channel network.

Title Page

Abstract

Introduction

Conclusions

References

Tables

Figures

◀

▶

◀

▶

Back

Close

Full Screen / Esc

Printer-friendly Version

Interactive Discussion



## Spatial and temporal pattern analysis of salt marsh evolution

A. Taramelli et al.

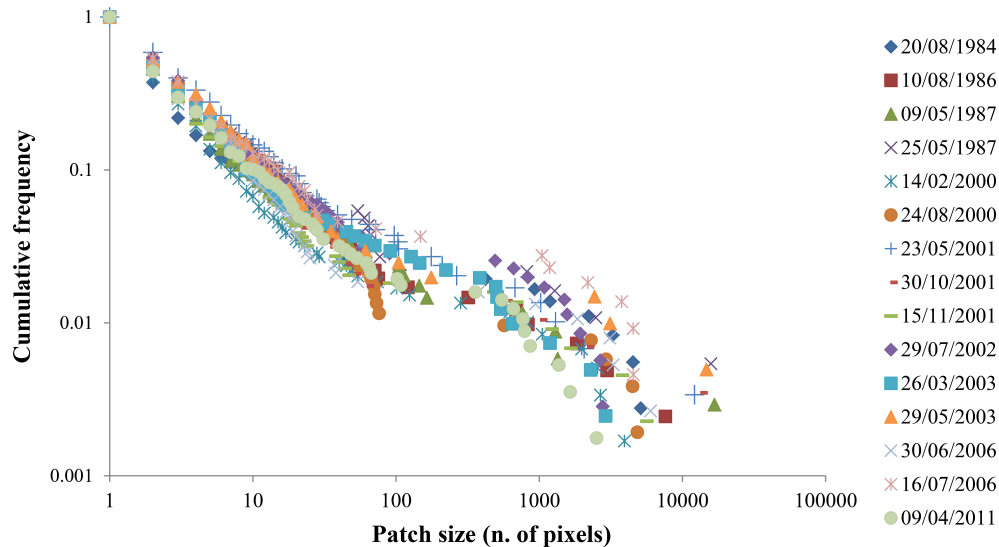


**Fig. 5.** Power law patch size distributions for the “High” vegetation class. A frequent deviation in the tail of the distributions – related to the largest patches – is observed in the dataset.

Title Page

Abstract

Introduction

Conclusions

References

Tables

Figures



Back

Close

Full Screen / Esc

Printer-friendly Version

Interactive Discussion



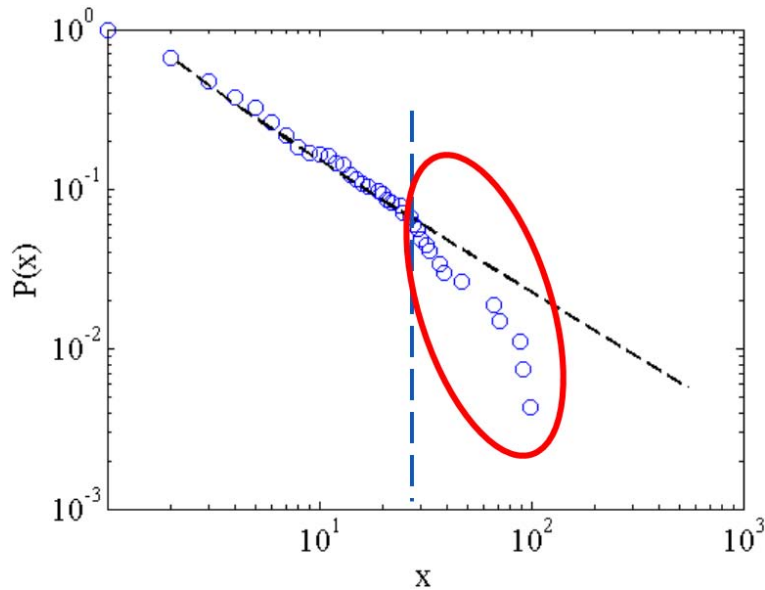


**Fig. 6.** Power law distribution for the Landsat acquisition of 24 August 2000.

**Spatial and temporal pattern analysis of salt marsh evolution**

A. Taramelli et al.

Title Page	
Abstract	Introduction
Conclusions	References
Tables	Figures
◀	▶
◀	▶
Back	Close
Full Screen / Esc	
Printer-friendly Version	
Interactive Discussion	



## Spatial and temporal pattern analysis of salt marsh evolution

A. Taramelli et al.

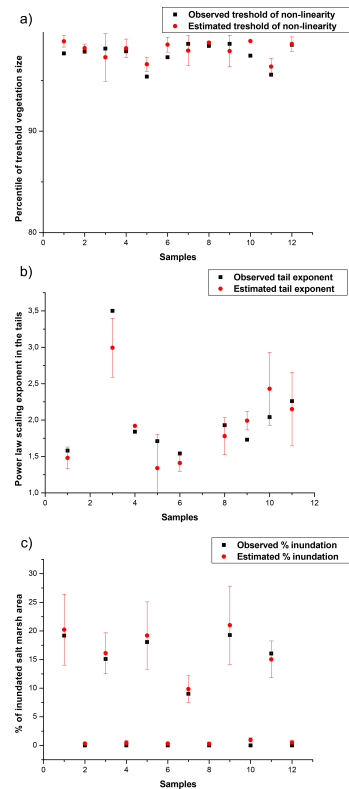


**Fig. 7.** Observed and estimated values for **(a)** the power law nonlinearity thresholds in the first step of the fuzzy Bayesian model (the threshold was transformed into the corresponding percentile in the whole distribution); **(b)** the power law scaling exponent in the tail of the original distribution, in the second step of the model; **(c)** the percentage of inundated salt marsh area in the third step of the model.

**Spatial and temporal  
pattern analysis of  
salt marsh evolution**

A. Taramelli et al.

Title Page

Abstract

Introduction

Conclusions

References

Tables

Figures

◀

▶

◀

▶

Back

Close

Full Screen / Esc

Printer-friendly Version

Interactive Discussion

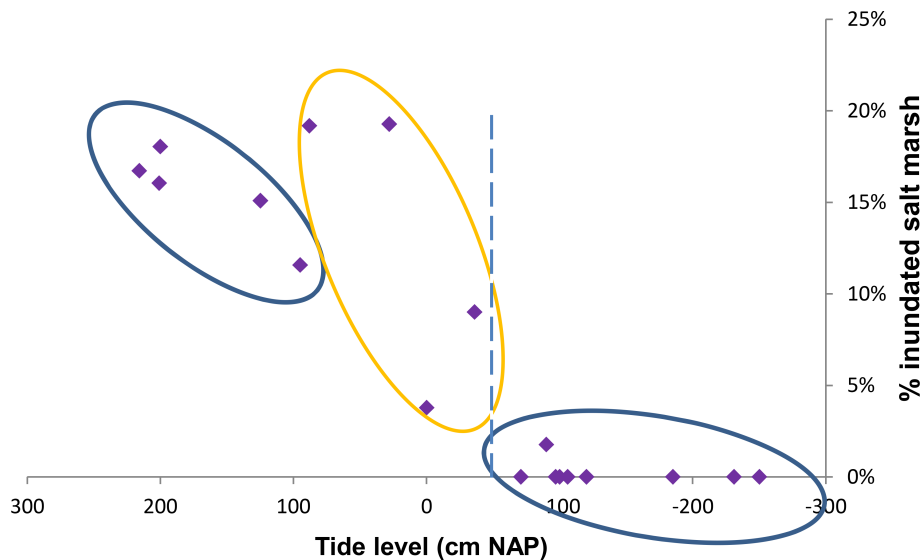


**Fig. 8.** Relationship between tidal level (cm NAP) and corresponding percentage of inundated salt marsh. The two variables appear to show a linear relationship until a tide level of  $-50$  cm, and again for tidal levels greater than  $95$  cm.